Scripta Materialia 161 (2019) 58–61

Contents lists available at ScienceDirect

Scripta Materialia

journal homepage: www.elsevier.com/locate/scriptamat

Regular article

The effect of size on the plastic deformation of annealed cast aluminium microwires

S. Verheyden *, L. Pires Da Veiga, L. Deillon, A. Mortensen

Ecole Polytechnique Fédérale de Lausanne (EPFL), CH-1015 Lausanne, Switzerland

ARTICLE INFO

Article history:
Received 14 August 2018
Received in revised form 1 October 2018
Accepted 8 October 2018
Available online 18 October 2018

Keywords:
Annealing
Aluminium
Size effects
Thermal activation
Monocrystalline

ABSTRACT

Monocrystalline, cast aluminium microwires of diameter (D) below 25 μm free of micromilling artefacts are annealed under protective atmosphere. Annealing increases the flow stress of all tested microwires, by an amount that is found, in a Haasen plot of measured activation area values, to be an athermal contribution to the flow stress that is attributed to surface oxide layer thickening. Microwires oriented for single slip with D ~14 μm behave as do as-cast microwires with D ~7 μm, showing a transition to higher and more stochastic flow stress values; this effect is attributed to a greater scarcity of dislocation sources after annealing.

Size-dependent plastic deformation is observed when the external dimensions of a sample decrease to approach and then fall below the length-scale of mechanisms that control plasticity in the material [1–8]. As the sample dimensions decrease one generally finds that: (i) the flow stress increases, (ii) the spread on the measured flow stress increases and (iii) the deformation behaviour becomes increasingly intermittent. Flow stresses are typically higher than the flow stress of the bulk single crystal but remain generally well below the theoretical strength of the material.

Annealing heat treatments are commonly used to lower the initial defect content of macroscale materials, making them softer and more ductile. Comparatively, annealing has rarely been applied at the microscale. Kiener et al. [9] annealed Cu micropillars to remove focused ion beam (FIB) induced damage present after sample production. They found that annealing leads to a marked increase in yield stress followed by softening. The appearance of a yield point was attributed to a lack of available dislocation sources upon initial deformation, such that yield stresses measured are characteristic of dislocation nucleation mechanisms. As the dislocation structure in the sample develops during deformation, flow stresses become similar to those in similarly deformed non-annealed samples. A similar observation was made in Ref. [10]. In contrast, studies on open-pore microcellular aluminium (foams) consisting of many monocrystalline struts of D < 100 μm showed softening following annealing, similar to aluminium bulk behaviour [11].

We explore here the influence of thermal annealing in microcast crystals of aluminium, which demonstrate a plasticity size effect yet are produced free of defects inherent to FIB-milling and allow probing, in uniaxial tension, a comparatively large sample volume. Cast aluminium microwires are annealed and their mechanical properties are compared with those of as-cast aluminium (99.99%) microwires characterized in Refs. [12,13].

The wires are produced through a microcasting process to feature a high aspect ratio (>30) and a tailored diameter (D) in the 7–120 μm range. The microwires are monocrystalline, with a random crystalline orientation, and are free of micromilling defects. The dislocation density of as-cast microwires was previously estimated using TEM to be around $1.2 \cdot 10^{11}$ m^{-2} [12]. More recently, using synchrotron X-ray Laue microdiffraction, the density of geometrically necessary dislocations was found in as-cast microwires to be around $8 \cdot 10^{11}$ m^{-2} [14]. When loaded in tension the microwires deform intermittently, the size of sudden displacement events following a power-law followed by a second, exponential, cut-off regime. The yield stress of the microwires scales roughly as D^{-1}.

For the work presented here fourteen monocrystalline aluminium (99.99%) microwires, all with D < 25 μm, were produced using the microcasting process of Ref. [12]. Prior to testing, each microwire was individually annealed under argon. All, except for two, microwires were then tested in tension following the methodology described in Ref. [12]. The two remaining microwires were tested with multiple single stress relaxations, following the testing and data interpretation methods described in Ref. [15]. We note in passing that separate tests have shown that there is no measurable influence of the stress relaxations on the deformation of the cast aluminium microwires [13].

* Corresponding author at: EPFL, STI, IMX, LMM, MXD 140, Station 12, CH-1015 Lausanne, Switzerland.
E-mail address: suzanne.verheyden@epfl.ch (S. Verheyden).

https://doi.org/10.1016/j.scriptamat.2018.10.009

The aluminium microwires are annealed while free-standing, or in other words after removal of the salt mould in which they were cast. For ease of manipulation the wire is glued to a tensile support using an alumina-based heat-resistant ceramic paint (989 alumina ceramic from Cotronic Corp). Each microwire is encapsulated in a Pyrex tube filled with 800 hPa argon to limit oxidation. In half the encapsulations a piece of titanium was added as an oxygen-getter; this introduced no marked difference on the microwire or its mechanical properties. The sealed encapsulation is heated to 500 °C for 2 h after which it is left to cool in the oven. After annealing, the wires are removed from the capsule and tested in tension following the procedures described in Refs. [12, 13, 15]. The adhesive forces of the alumina glue are insufficient for tensile testing; therefore, after annealing the microwires are re-glued to the support using Loctite 496™.

Even though the heat-treatment was performed under a protective atmosphere of argon, SEM images show that a visible surface oxide layer has grown along their surface (with as-cast microwires the oxide was not observable in the SEM, Fig. 1b), and this is independent of whether a titanium oxygen getter was placed next to the sample upon encapsulation. The actual oxide thickness of the annealed microwires is estimated to be around 20 nm based on SEM images. This value is consistent with literature data: Beck et al. [16] measured a maximum oxide thickness of 20 nm after exposure of aluminium to 500 °C in a 100 hPa O^2 atmosphere, these being conditions that match closely those of the present experiments. By contrast, as-cast microwires are expected to have an oxide layer thinner than 10 nm [17], which agrees with the fact that this layer could not be observed on the SEM images of deformed as-cast microwires. We neglect hereafter any difference in oxide layer thickness with microwire diameter or orientation, as a difference in oxide thickness with aluminium free surface crystallographic orientation has only been documented for longer (>2 h) elevated temperature exposure times [18].

Deformation of the wires proceeds, as is the case for as-cast microwires, largely through sudden displacement bursts, or in other words intermittently. Fig. 1a shows a 14 μm microwire oriented for single slip after testing: one glide system was primarily activated in this wire, and both large and small slip steps are visible along its surface. Although a full statistical analysis was not performed, the size of the slip steps along the deformed annealed wires falls within the size-range of detected sudden displacement events, shown in Fig. 3a.

Fig. 2 shows the shear strain and stress curve of ~14 μm and ~23 μm microwires respectively. As was the case for as-cast microwires, the

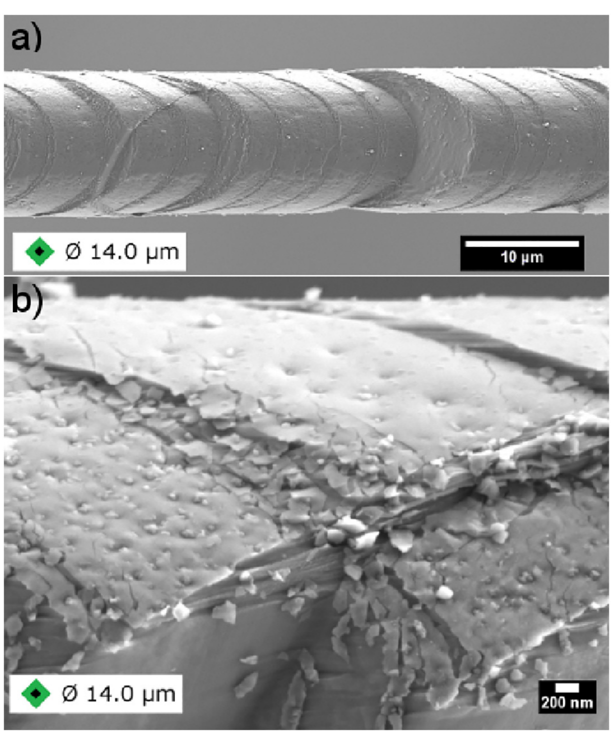

Fig. 1. a) SEM image showing slip steps at the surface of an annealed single slip oriented microwire after testing, b) higher magnification of the surface of the microwire shows fragments of an oxide layer around a slip step.

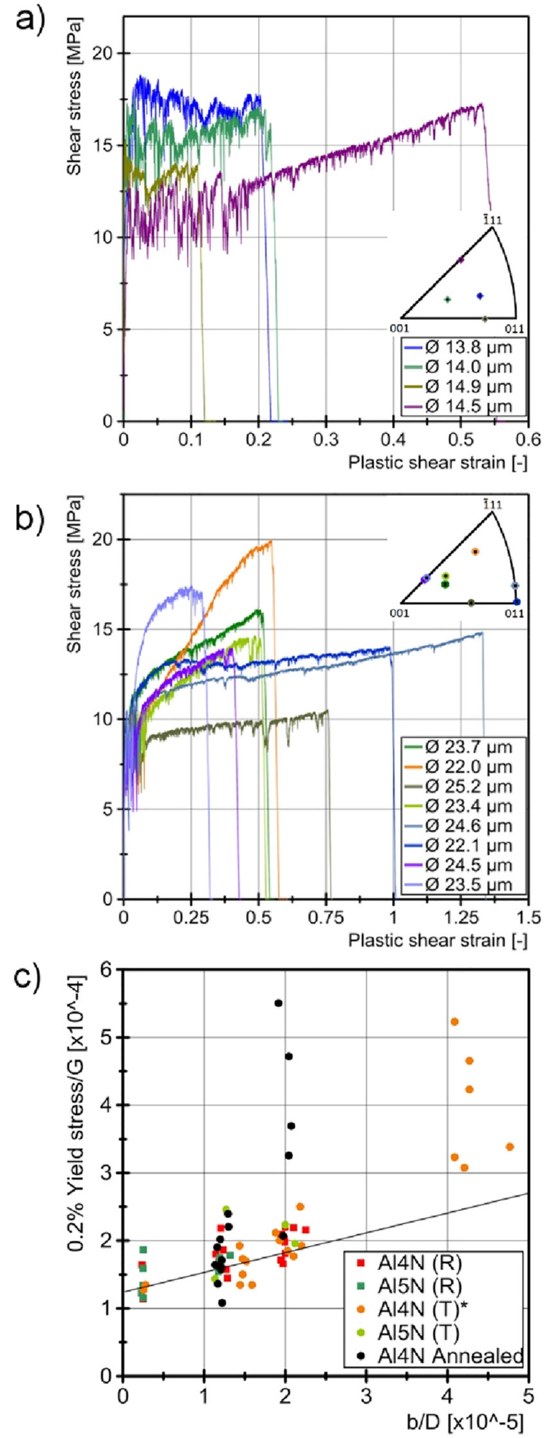

Fig. 2. Resolved plastic shear stress vs. resolved shear strain plot of annealed microwires tested in tension with a diameter of a) ~14 μm and b) ~23 μm respectively. The crystallographic orientation of the microwires is shown in the standard triangle given as inset. c) 0.2% Yield stress normalized by the shear modulus *G* versus the inverse of the crystal diameter normalized by the Burgers vector. The linear trend line is based on a single-arm source model described in Ref. [12]. Coloured data points are taken from Refs. [12,13,15]; (T) denotes data from monotonic tensile testing; (R) denotes data from tests that included relaxation testing; 4 N and 5 N give the metal purity.

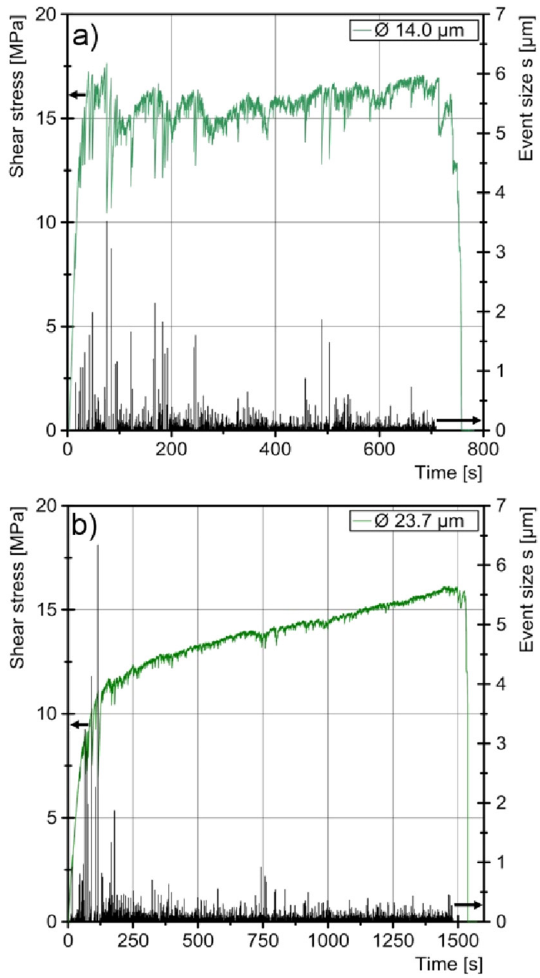

Fig. 3. Shear vs. time for an single slip oriented annealed microwire of diameter of a) 14.0 μm and b) 23.7 μm respectively and a common crystallographic orientation. The size of detected displacement events is plotted in parallel to illustrate how magnitude and distribution in time of detected drops differ as the microwire diameter changes from 14 to 24 μm.

plastic deformation behaviour of the annealed microwires depends strongly on their diameter. Considering microwires oriented for single slip (orientation within the standard stereographic triangle) there is a distinctive difference, in both the yield stress and the overall plastic deformation, between ~14 and ~23 μm microwires. Similar to what has been observed in literature for annealed micro-milled samples, ~14 μm microwires have a significantly higher flow stress compared to as-cast microwires of similar diameter and orientation (Fig. 2c, see also [12,13]). Comparing with as-cast microwires, the measured tensile flow stresses reach, after annealing, the range of values that were previously measured for 7 μm diameter as-cast microwires [12].

Contrary to what is presented in the literature for other annealed microsamples, the increase in yield stress that is brought here by annealing is not accompanied by the appearance of a yield point or followed by extensive softening; instead, as deformation continues, the (highly irregular) annealed microwire flow stress remains noticeably above values measured for as-cast microwires. Present observations differ also from what was found with the same metal in replicated microcellular form, which shows a classical softening behaviour after annealing in flowing Ar at 500 °C for 2 h [11].

The ~14 μm annealed microwires oriented for single slip have strain-to-failure values that are highly variable and that tend to be lower than values found in their as-cast counterpart (see the supplementary online material for a graphical comparison). The deformation of those microwires progresses through large sudden displacement events interspersed with smaller events (Fig. 2a) up to sudden failure. Intermittency of deformation is also increased after annealing: with as-cast ~14 μm microwires, sudden displacement events larger than 1 μm were rarely observed [12,13].

Annealing has a different effect on deformation of the ~23 μm microwires: (i) yield stress values remain closer to what was measured for as-cast microwires of the same size (Fig. 2c), (ii) large (>1 μm) sudden displacement events are measured only at the onset of intermittent plasticity, which transits into a quieter regime after a small finite amount of deformation (Fig. 2b), (iii) all annealed microwires tend on average to deform to higher (not lower) strains than do their as-cast counterparts.

The tensile curve of the double-slip oriented 14.5 μm microwire follows more closely the behaviour observed for the 23 μm microwires (including a lower yield stress), pointing to an influence of both size and the number of activated slip systems on the influence that annealing exerts on the plastic deformation of the microwires.

Part of the observed results can be attributed to the thicker oxide layer formed during annealing. Before the detection of the first displacement event, but after yield, a period of rapidly rising, yet smooth, flow stress is measured for all annealed microwires. A similar initial smooth and rapid increase in flow stress was previously found by Ngan et al. [19] in the deformation of aluminium micropillars coated with a layer of tungsten, where it was found that upon initial deformation, dislocations are trapped within the volume and pile-up at the surface layer. The same interpretation can account for present data, with the oxide layer playing the same role as the tungsten coating did for FIB-machined micropillars.

Relaxation data are informative in this regard, as they can detect the presence of an athermal stress component to the overall flow stress. One ~14 and one ~23 μm microwire, both oriented for single slip, were thus tested with multiple 60 s long stress relaxations. Their tensile curves are given in Fig. 4a, where the black inverted triangles on the curve mark the point at which a stress relaxation was performed. The thermally activated deformation behaviour of as-cast microwires combines continuous relaxation with sudden displacement events. As a result, one must separate the intermittent part of the signal to measure the (apparent) activation area characteristic of continuous relaxation processes. The method developed to this end is described in Ref. [15]; it consists of 3 main steps: (1) binning the stress relaxation to smoothen the time-derivative, (2) discarding bins that correspond to sudden displacement jumps and (3) calculating the apparent activation area based on the remaining bins.

In Fig. 4b the calculated apparent activation areas are shown in a Haasen plot. As seen, 14 μm and the 23.7 μm microwire data are similar within accuracy of the measurement. For both microwires the activation area is constant over an initial stress interval ($\tau < 10$ MPa). In the stress-strain curve this corresponds to the initial region of smooth increase in flow stress. This is explained as a regime of back-stress build-up within the microwire, during which the overall internal state of the microwire does not change significantly. In the second part ($\tau > 10$ MPa) of the thermally activated deformation data, a linear fit through data points in the Haasen plot gives (i) a slope that is similar to what was previously measured for single slip as-cast microwires of similar diameter [13] and (ii) a positive intercept with the stress-axis at ≈9.5 MPa for both the 23.7 μm and the 14.0 μm microwire. This shift in stress-axis intercept matches the average difference in flow stress measured between as-cast and annealed microwires. We thus conclude that the difference in initial flow stress that comes after annealing corresponds to an athermal contribution to the flow stress, itself due to the presence of a thicker oxide layer along the wire surface.

In as-cast microwires, a transition to higher and more stochastic yield stress values, and generally lower tensile failure strain, is observed as the wire diameter of single-slip wires falls to values near 7 μm [12] (see also Fig. 2c). This transition is attributed to the fact that, at this diameter (and below), well-oriented glide dislocation sources become scarce in the crystal [20]. This causes the stress required (on average) for dislocation glide and multiplication to increase and show a greater

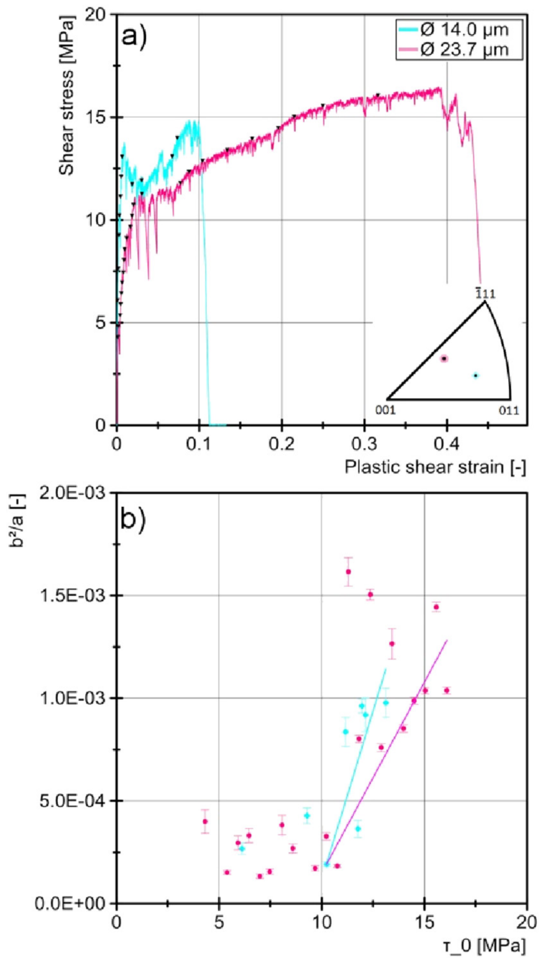

Fig. 4. (a) Stress-strain plot of 14.0 µm and 23.7 µm microwire tested with stress relaxation events; the point at which each 60 s stress relaxation was performed is marked by an inverted triangle on the curve. (b) The Haasen plot derived based on the binning technique for the same microwires (for a description of the binning technique see Ref. [13]).

degree of stochasticity, increasing in turn the probability that the wire will shear locally to the extent where it fails. Annealing generally lowers the initial dislocation density: with a lower initial dislocation density, it is expected that the wire diameter at which this transition (to a higher flow stress, greater stochasticity and generally lower failure strain) takes place will increase, roughly in proportion to the inverse square root of the initial dislocation density. This is indeed observed: after annealing, the transition to far higher and more stochastic yield stress values is now found in 14 µm single-slip wires, as opposed to 7 µm single-slip wires in the as-cast condition, Fig. 2c, suggesting in turn that the initial dislocation density has fallen by roughly a factor four after annealing (since the transition length scale has roughly doubled). The effect is expected to be stronger in single slip oriented microwires compared to double slip oriented microwires. Effectively, when considering only the yield stress values, the 14 µm microwire oriented for double slip has a markedly lower yield stress than do its single slip oriented counterparts.

A lack of readily available dislocation sources is also reflected in the overall shape of the tensile curve of ~14 µm annealed microwires compared to ~23 µm annealed microwires. For all tested ~23 µm annealed microwires, the appearance of large (>1 µm) slip events is limited to a small range of low strain values. This initial deformation stage is furthermore associated with the motion of a visible deformation front along the microwire length, which can be observed through reflection changes along the microwire during testing (see online Supplementary information). In the ~23 µm microwires, sufficient dislocations thus appear to be present for the early activation of slip. With 14 µm diameter microwires, on the other hand, such a propagating band of slip activation is not seen, slip occurring at more random locations from the beginning of the test onwards (see online Supplementary information).

In conclusion, we show that annealing cast aluminium microwires of diameter below 25 µm causes (i) an increase in the athermal component of the flow stress and (ii) an increase from 7 to 14 µm in the wire diameter below which deformation transits to higher, more stochastic yield stress values and lower average failure strain values. The former effect is attributed to an increase in the surface oxide layer thickness. The latter effect is attributed to a decrease (by a factor around four) in the initial dislocation density present within the wires. Below a size on the order of 10 µm, thus, the effect of annealing on plastic deformation of pure aluminium can be the inverse of what is observed with bulk metal samples.

We thank Dr. K. Schenk at EPFL for measuring the orientation of the microwires. The work described in this paper was supported by the Swiss National Science Foundation (Project No. 200020_156054/1).

Appendix A. Supplementary data

Supplementary data to this article can be found online at https://doi.org/10.1016/j.scriptamat.2018.10.009.

References

[1] E. Arzt, Acta Mater. 46 (1998) 5611–5626.
[2] J.G. Sevillano, I. Ocaña Arizcorreta, L.P. Kubin, Mater. Sci. Eng. A309–310 (2001) 393–405.
[3] J.A. El-Awady, Nat. Commun. 6 (2015) 5926.
[4] G. Dehm, B.N. Jaya, R. Raghavan, C. Kirchlechner, Acta Mater. 142 (2018) 248–282.
[5] P. Zhang, O.U. Salman, J.-Y. Zhang, G. Liu, J. Weiss, L. Truskinovsky, J. Sun, Acta Mater. 128 (2017) 351–364.
[6] L.P. Kubin, Dislocations, Mesoscale Simulations and Plastic Flow, 1 ed. Univ. Press, Oxford, 2013.
[7] J.R. Greer, J.T.M. De Hosson, Prog. Mater. Sci. 56 (2011) 654–724.
[8] O. Kraft, P.A. Gruber, R. Mönig, D. Weygand, Annu. Rev. Mater. Res. 40 (2010) 293–317.
[9] D. Kiener, Z. Zhang, S. Šturm, S. Cazottes, P.J. Imrich, C. Kirchlechner, G. Dehm, Philos. Mag. 92 (2012) 3269–3289.
[10] J.M. Wheeler, C. Kirchlechner, J.-S. Micha, J. Michler, D. Kiener, Philos. Mag. 96 (2016) 3379–3395.
[11] R. Goodall, J.-F. Despois, A. Mortensen, Scr. Mater. 69 (2013) 469–472.
[12] J. Krebs, S.I. Rao, S. Verheyden, C. Miko, R. Goodall, W.A. Curtin, A. Mortensen, Nat. Mater. 16 (2017) 730–736.
[13] S. Verheyden, L. Deillon, A. Mortensen, (Submitted).
[14] L. Deillon, S. Verheyden, D. Ferreira Sanchez, S. Van Petegem, H. Van Swygenhoven, A. Mortensen, (In Progress).
[15] S. Verheyden, L. Deillon, A. Mortensen, Data Brief (2018) (submitted for publication).
[16] A.F. Beck, M.A. Heine, E.J. Caule, M.J. Pryor, Corros. Sci. 7 (1967) 1–22.
[17] F. Diologent, R. Goodall, A. Mortensen, Acta Mater. 57 (2009) 286–294.
[18] J.I. Eldridge, R.J. Hussey, D.F. Mitchell, M.J. Graham, Oxid. Met. 30 (1988) 301–328.
[19] K.S. Ng, A.H.W. Ngan, Acta Mater. 57 (2009) 4902–4910.
[20] L. Johnson, M. Ashby, Acta Metall. 16 (1968) 219–225.